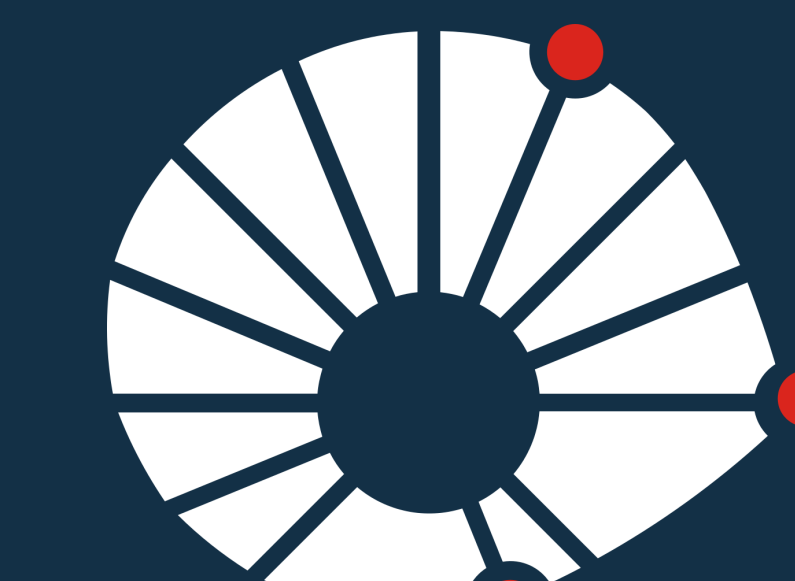


DEVELOPMENT OF HIGH-ORDER $H(\text{curl}, \Omega)$ -CONFORMING APPROXIMATION SPACES FOR PHOTONIC WAVEGUIDE ANALYSIS

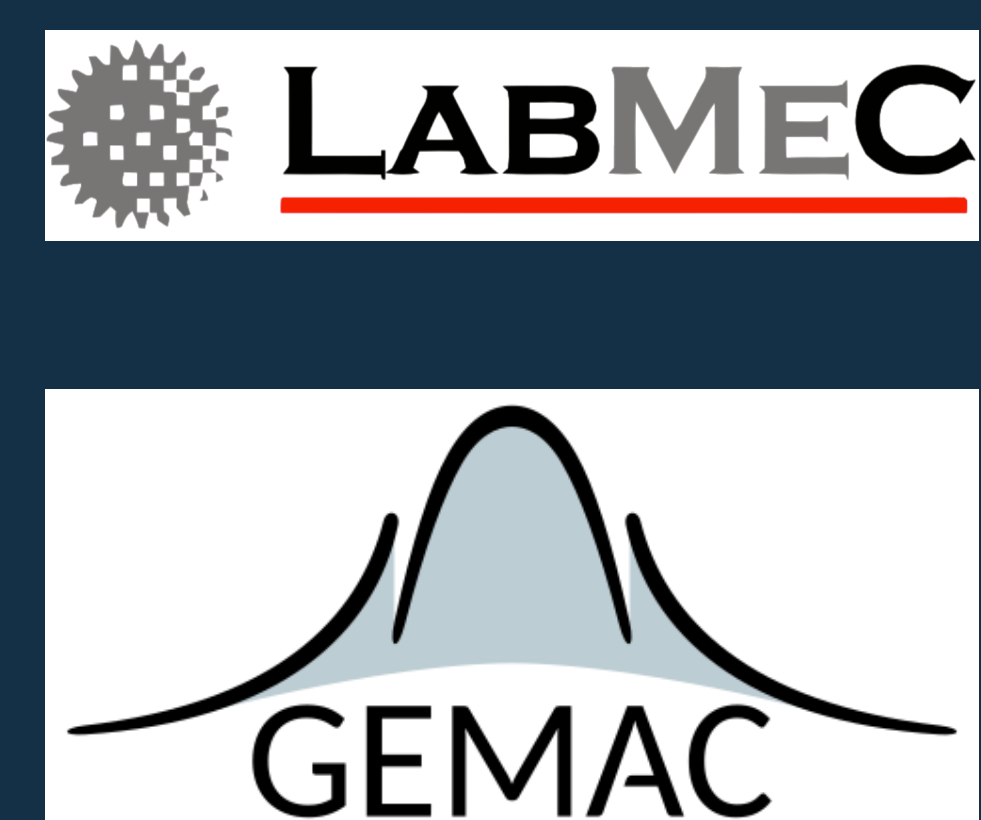
Francisco T. Orlandini¹, Hugo E. H. Figueira¹ and Philippe R. B. Devloo²

¹School of Electrical and Computer Engineering, State University of Campinas, Brazil

²School of Civil Engineering, Architecture and Urban Design, State University of Campinas, Brazil



UNICAMP



1. MOTIVATION

The design of photonic waveguides requires a high degree of precision on the dispersion parameters. Such requirement has led the Computational Electromagnetics(CE) community to seek a diversity of numerical methods, such as the pseudospectral methods. In this work it is shown that the Finite Element Method(FEM) is capable of achieving that precision in an efficient way if high-order elements, not very popular in the CE community, are used. The conditions for benefiting from the higher convergence rates are exposed and real-world scenario results are presented exemplifying the use of hp-adaptive finite elements.

2. FEM FORMULATION AND THE $H(\text{curl}, \Omega)$ -CONFORMING ELEMENTS

The formulation used in this work performs modal analysis on the cross-section Ω of a waveguide for a given angular frequency ω , using $H(\text{curl}; \Omega)$ and $H^1(\Omega)$ -conforming elements for the transverse and longitudinal components of the electric field, respectively. It is valid for a domain composed of materials presenting at most transverse-anisotropy. From Jin [1]: Find non-trivial $(\beta^2, e_t, e_z) \in (\mathbb{C} \times [\mathbb{C}]^N \times [\mathbb{C}]^M)$ such that:

$$\int_{\Omega} \left\{ \sum_j^N e_{tj} [\mu_{zz}^{-1} (\nabla_t \times \varphi_j) \cdot (\nabla_t \times \varphi_i)^* - k_0^2 \epsilon_{xy} \varphi_j \cdot \varphi_i^*] + \beta^2 \sum_l^M e_{zk} \left[\sum_j^N e_{tj} \mu_{xy}^{-1} (\nabla_t \varphi_k + \varphi_i) \cdot (\nabla_t \varphi_k + \varphi_i)^* - k_0^2 \epsilon_{zz} \varphi_k \varphi_k^* \right] \right\} d\Omega = 0, \quad (1)$$

$\forall \varphi_j \in B_{U_h}, \varphi_k \in B_{V_h}$,

where B_{U_h} and B_{V_h} denote the FEM basis for the finite-dimensional subspaces of $H(\text{curl}; \Omega)$ and $H^1(\Omega)$, respectively.

The $H(\text{curl}; \Omega)$ -conforming elements used in this work are the Nédélec elements of the first kind Nédélec [2] and were constructed in the NeoPZ framework in a hierarchical way.

3. EFFECTS OF GEOMETRICAL REPRESENTATION

In order to benefit from the high-order elements, non-linear mapped elements are essential when dealing with curved geometries. Figure 1 compares the convergence rate of the effective index n_{eff} for a step-index optical fiber with polynomial order $k = 4$, using three different types of mapped elements.

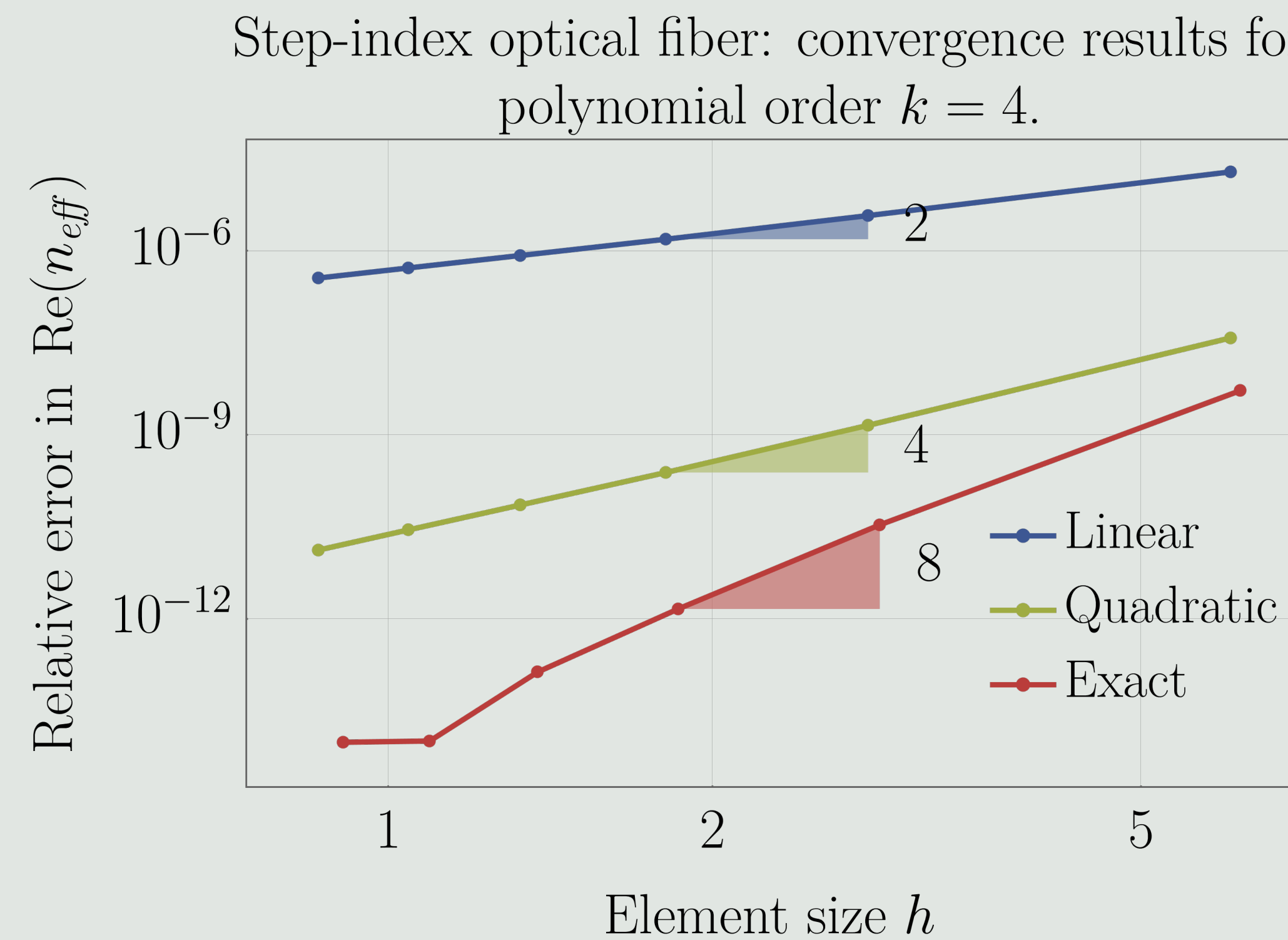


Figure 1: Comparison of convergence rates for the real part of the effective index of a step-index optical fiber. The polynomial order $k = 4$ was used in all three approximations. The geometry was described with elements obtained by linear mapping(blue curve), quadratic mapping(green curve) and exact mapping(red curve).

The optimal convergence rate is only obtained with the non-linear mapping: with a fixed number of elements, the linear mapping achieved an error of 10^{-6} , the quadratic mapping obtained 10^{-9} , and a relative error of 10^{-13} was obtained with the exact mapped elements. Figure 2 shows two Linear Polarized modes on the step-index optical fiber.

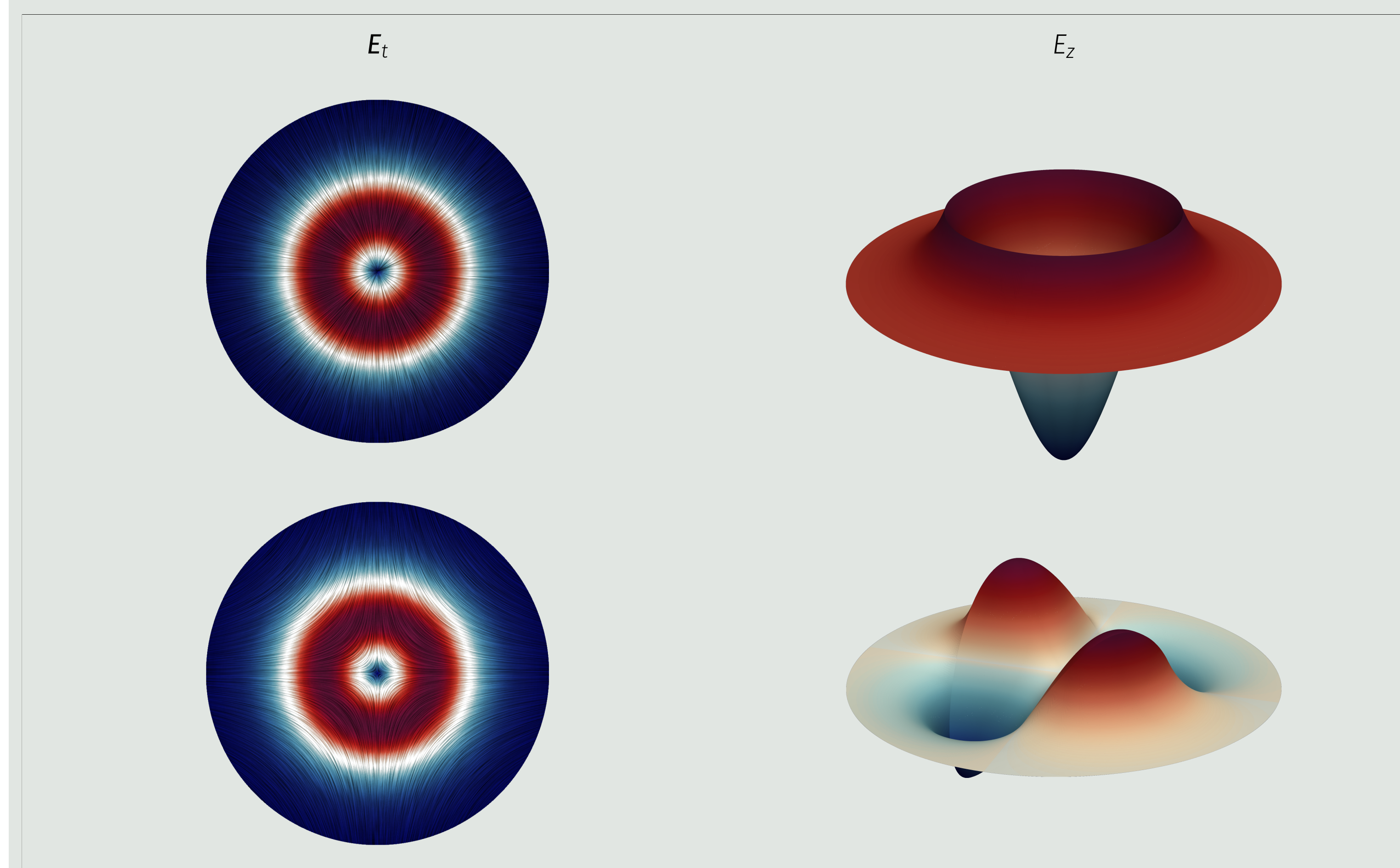


Figure 2: The first four approximated LP modes for a step-index optical fiber with $r_{\text{core}} = 8\mu\text{m}$ and refractive indexes $n_1 = 1.4457$ (core) and $n_2 = 1.4378$ (cladding). The fiber is analyzed for $\lambda_0 = 1.55\mu\text{m}$. On the left, the Line Integral Convolution of the transversal component of the electric field is shown, and on the right its correspondent longitudinal component.

4. HP-ADAPTIVITY CAPABILITIES

The developed basis functions, due to the hierarchical construction, can be integrated in the hp -algorithms of the NeoPZ framework[3].

Figure 3 shows a hp -adaptive mesh, in which the refinements were performed upon observation of the solution obtained with a fine mesh.

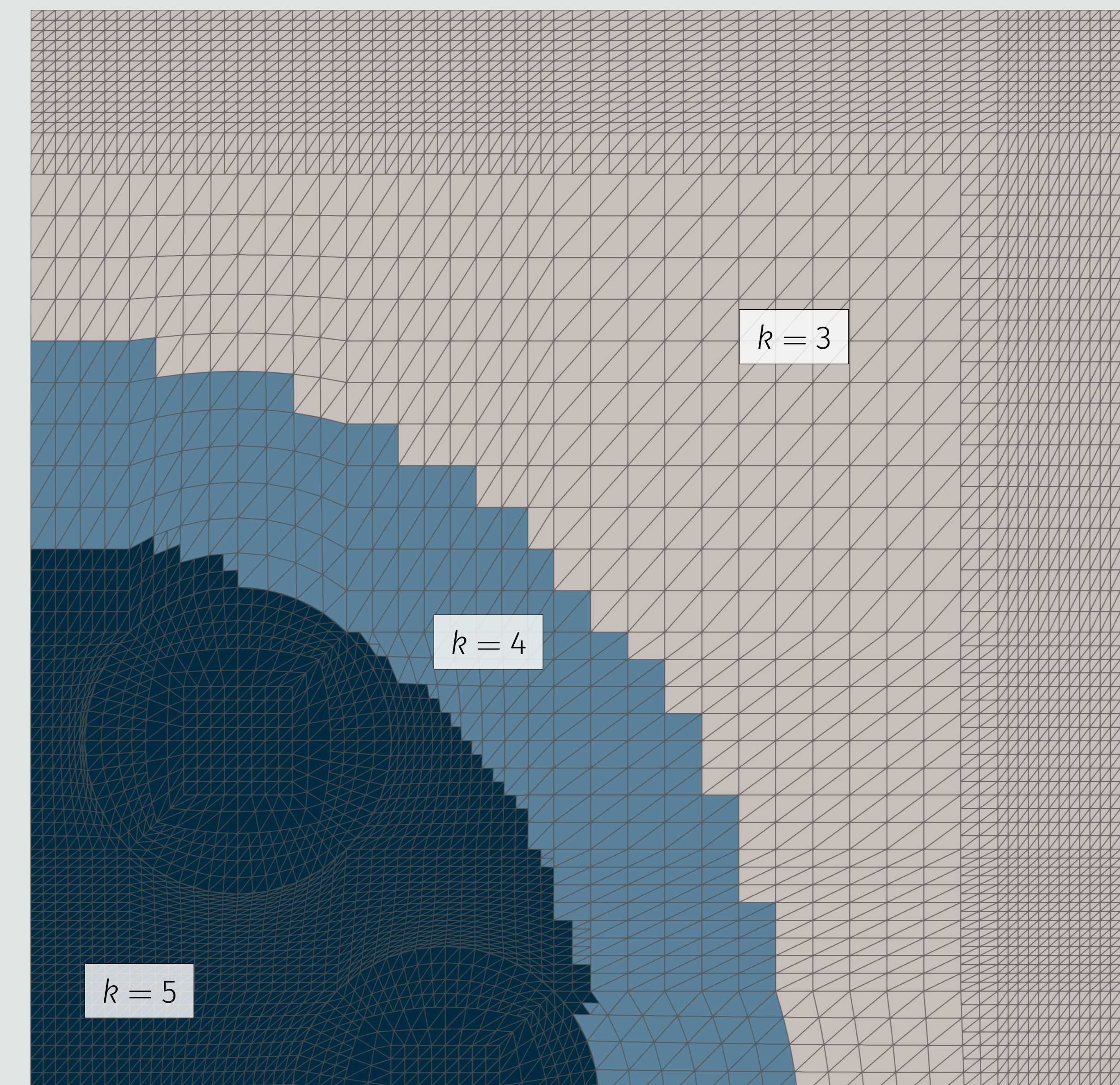


Figure 3: The Finite Element mesh of the microstructured fiber with six air-holes. The waveguide has a hole diameter of $d = 5\mu\text{m}$ and a hole pitch of $\Lambda = 6.75\mu\text{m}$. The computational domain takes advantage of the symmetry of the desired fields and is a square with side $l = W + d_{\text{pm}}$, with $W = 15.75\mu\text{m}$ and $d_{\text{pm}} = 2\mu\text{m}$. The elements have varying polynomial order from $k = 3$ to $k = 5$, and the mesh was refined on the region near the holes.

Finally, Figure 4 shows the electric field plots obtained with the mesh of Figure 3.

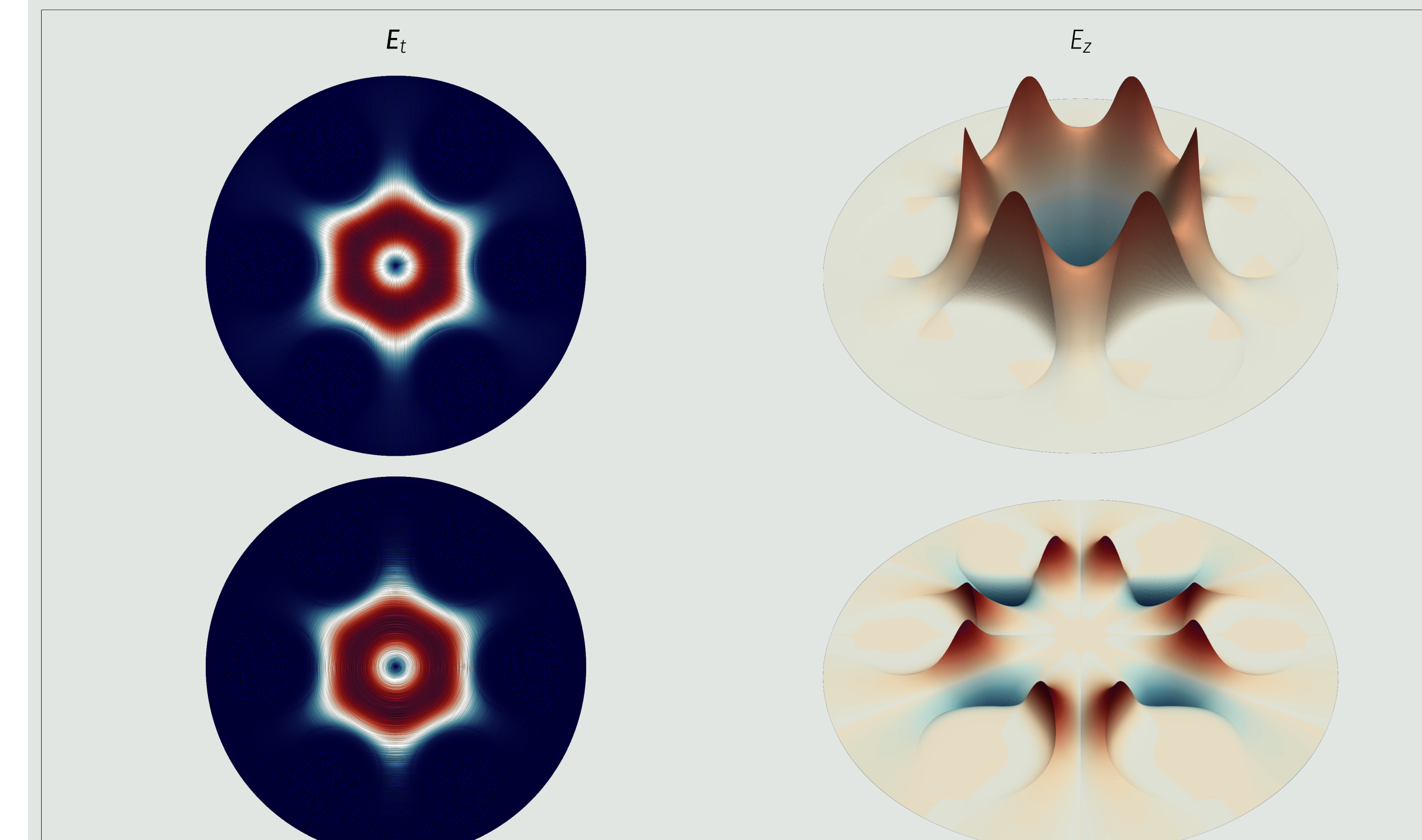


Figure 4: Electric field plot of the sixth(up) and third(down) non-degenerated electromagnetic modes of the microstructured fiber. On the left, the Line Integral Convolution of the transversal component of the electric field is shown, and on the right its correspondent longitudinal component.

REFERENCES

- [1] J.-M. Jin, *The Finite Element Method in Electromagnetics*. Wiley-IEEE Press, 2014.
- [2] J.-C. Nédélec, "Mixed finite elements in \mathbb{R}^3 ", *Numerische Mathematik*, vol. 35, no. 3, pp. 315–341, Sep. 1980.
- [3] J. L. D. Calle, P. R. Devloo, and S. M. Gomes, "Implementation of continuous hp-adaptive finite element spaces without limitations on hanging sides and distribution of approximation orders", *Computers & Mathematics with Applications*, vol. 70, no. 5, pp. 1051–1069, 2015.